A New Method for Efficient Global Optimization of Large Systems Using Sub-models

HEEDS COMPOSE demonstrated on a crash optimization problem

Nate Chase, Ranny Sidhu, Ron Averill
Red Cedar Technology
4572 S. Hagadorn Rd.
Suite 3-A
East Lansing, MI 48823

Abstract

Executing full vehicle finite element simulations can be very time consuming and expensive. Compound this with the large number of evaluations required for crash optimization problems due to their complicated design landscapes, and optimization of full vehicle crash simulations becomes very computationally expensive and difficult. An ideal solution is to reduce the full vehicle down to a manageable sub-model which runs significantly quicker while maintaining the boundary constraints as if utilizing the full vehicle model. The optimization process can then be managed with this sub-model while achieving significant improvements in computational requirements.

*This paper will demonstrate how to optimize the a-pillar, b-pillar, roof rail, rocker, front header, and roof bow components of a car for roof crush, utilizing Ultra High Strength materials. In addition to the gauge of the individual structural components, a soft zone trigger and its location within the b-pillar are introduced as design variables. LS-DYNA® is utilized as the simulation tool with the new COMPOSE (**COMP**onent **O**ptimization in a **S**ystem **E**nvironment) feature within the HEEDS-MDO optimization software utilized to perform the optimization. COMPOSE is a new module that enables the use of a sub-model for optimization in a way that significantly reduces the overall optimization time while encouraging the interactions of the optimal subsystem with the global model to be consistently maintained. This creates a design that gives a similar high performance in the global model as was found in the sub-model.*

It is shown here that the use of COMPOSE can significantly decrease the design time for finding high performing designs for the roof crush optimization, over a traditional global optimization approach. In addition, it is shown that performing an optimization on the sub-system level by using the original boundary conditions from the global model is not a robust approach for this optimization. The study shows that to take advantage of the reduced runtime in the sub-system model, the COMPOSE technology provides a robust solution for efficient optimization of the system.

Introduction

Executing full vehicle finite element analyses can be time consuming and expensive. Compound this with the fact that crash optimization problems require a large number of evaluations (due to the complicated design landscape), and optimization of full vehicle crash simulations becomes computationally costly and difficult. An ideal solution is to reduce the full vehicle model down to a manageable sub-model that can be analyzed much more quickly, while maintaining the boundary constraints as if using the full vehicle model. The optimization process can then be managed with this sub-model while significantly reducing the computational requirements.

This paper will demonstrate how to optimize the A-pillar, B-pillar, roof rail, rocker, front header, and roof bow components of a car for roof crush, utilizing ultra-high-strength steel. In addition to the gauge of the individual structural components, a soft zone trigger and its location within the B-pillar are introduced as design variables. LS-DYNA® [1] is utilized as the simulation tool with the COMPOSE (**COMP**onent **O**ptimization in a **S**ystem **E**nvironment) module for HEEDS MDO used to perform the optimization.

COMPOSE enables the use of a sub-model for optimization in a way that significantly reduces the overall optimization time. Using COMPOSE, the majority of the evaluations during the optimization are performed using the sub-model, while only a handful of full model evaluations are performed to maintain the coupling between the two models.

Challenges of System Design Optimization

The objective of a system design optimization is to find the design that behaves the best in a given environment under a set of prescribed conditions. However, design optimization of automotive systems undergoing roof crush requires many large-scale, nonlinear finite element simulations. Often it is not practical to perform design optimization on large automotive structures, due to the analysis time required to perform so many design evaluations. The introduction of COMPOSE makes these complex optimizations feasible in a realistic timeframe. [2]

The use of sub-models is not a new concept. But, because the performance of the sub-system relies on the boundary conditions from the global system model, the optimization process needs to identify both the sub-system design that is optimal under certain conditions and the boundary conditions that allow the sub-system to behave optimally.

This creates a challenge because the optimal design boundary conditions are not known *a priori*. Thus, they cannot be found until the design approaches its optimal form. Often a sub-system design will look great following a sub-system optimization process, only to perform poorly when used in the global system model. Simply because the sub-system design is optimal for a given set of boundary conditions doesn't imply that it works well for all boundary conditions. The COMPOSE module for HEEDS MDO is a direct iterative approach to solving these types of problems without the need for sensitivity derivatives.

Global Roof Crush Analysis and Design Models

A Ford Taurus-V2 LS-DYNA model [3] was adapted for use as the global model in this roof crush application (shown in Figure 1).

The gross vehicle weight (GVW) of the car being designed was 19.708 kN. The baseline simulation model had a total structural mass of 1.392 tonnes. The roof crush event was simulated as a 75 ms event by using a rigid impactor to crush the roof on the driver's side of the vehicle, as shown in Figure 1. The impactor was moved at a constant velocity of 2 m/s, normal to the impactor. The vehicle was constrained in DOF 1,2,4,5,6 at the vehicle hubs and DOF 3,4,5,6 at the rockers, as shown in Figure 2.

The material and gauge for most of the car components were the same as the Taurus-V2 model. The components that take the majority of the load during the roof crush event (A-pillar, B-pillar, roof rail, rocker, front header, and roof bow components, as shown in Figure 3) were changed to ultra-high-strength materials. The thickness of these components was modified during optimization to improve crash performance and decrease mass.

a. *Top view of global roof crush model.*

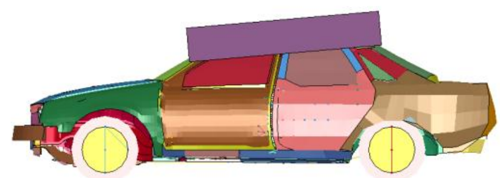

b. *Side view of global roof crush model.*

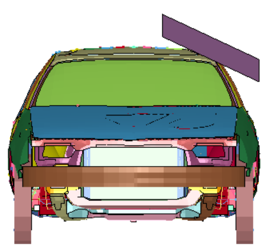

c. *Front view of global roof crush model.*

Fig.1 *Global LS-DYNA roof crush model.*

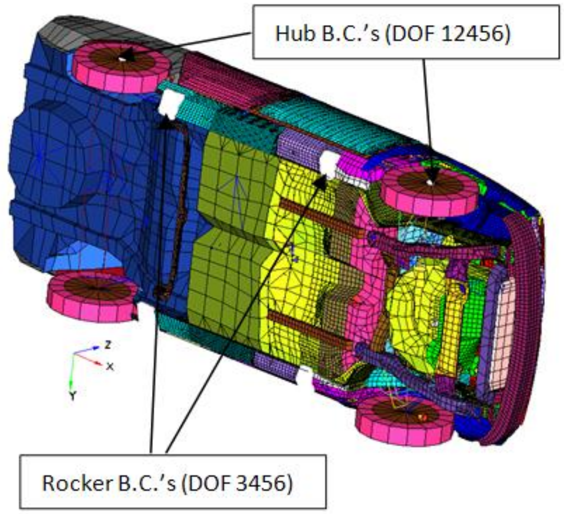

Fig.2. *Highlighted boundary condition locations at the hubs and rockers (symmetric cross-car).*

The parts of the structure that used ultra-high-strength materials were hot-stamped, boron-alloyed steels. Hot-stamped parts tend to provide better formability at higher temperatures, with the added bonus of no spring back on the final part [4].

Before hot-stamping, the base material in hot-stamped boron-alloy steels has a tensile strength of approximately 600 MPa. After a part is hot-stamped, its strength can increase by up to 250 percent; the hot-stamping process transforms the base material from a ferritic-pearlitic microstructure to a martensitic microstructure [5].

The example in Figure 4 compares the stress-strain curves of a typical high grade steel with that of a typical boron-alloyed steel that has been hot-stamped.

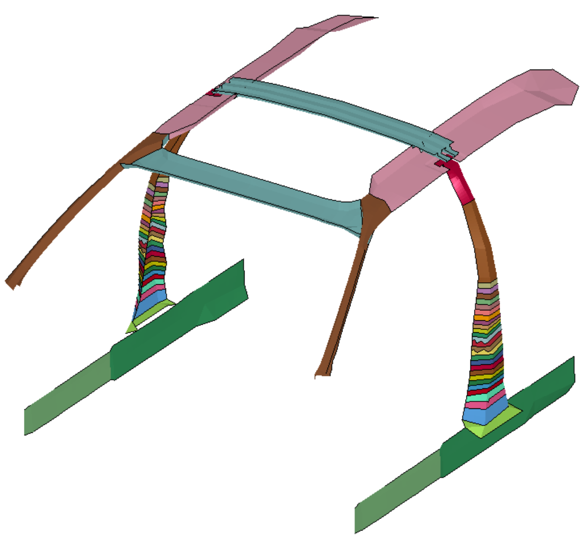

Fig.3. *Components made from Ultra High Strength materials in the automotive structure.*

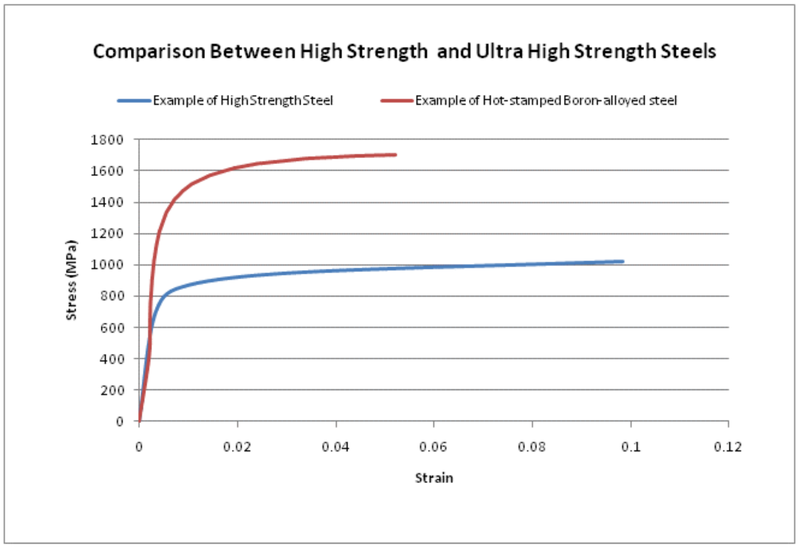

Fig.4. Comparison of typical stress-strain curves for high strength steel and hot-stamped boron-alloyed steel.

Roof Crush Sub-model for use with COMPOSE

The speedup in the optimization runtime achieved by COMPOSE depends on the ratio of the time it takes to run the global model to the time it takes to run the local model. The higher this factor, the larger the speedup you can expect with COMPOSE. As a result, the selection of the sub-model is an important step.

The sub-model is a smaller model (in spatial or time domain) that contains the variables to be optimized. The regions where parts are deleted to create the sub-model from the global model are called interface boundaries. The sub-model is analyzed by imposing the boundary conditions from the global model at the interface boundaries of the sub-model. HEEDS COMPOSE drives the sub-model by imposing the boundary conditions on the interface nodes directly in the input file.

Since sub-models have fewer total number of elements than global models (smaller model), they typically run much faster than the global models. Therefore, as long as the boundary constraints for a given sub-model match the global design, a representative solution can be found in less time by analyzing the sub-model instead of the global model.

The issue, of course, is that the boundary constraints on the sub-model cannot be guaranteed to match that of the global model without actually running the global model. If the boundary constraints applied to a given design are no longer valid when a modification is made that alters the design (such as during optimization), then the sub-model no longer represents the global model solution. However, there’s no way to know whether the boundary constraints are still valid until the new global analysis is performed. This is the dilemma COMPOSE helps to overcome.

To create a sub-model, a boundary cut is typically made to the global model outside the critical region of interest, creating the interface boundaries. Figure 5 shows the boundary cut made to the global roof crush model used in this study.

Since it is known that the primary structural members around the roof (A-pillar, B-pillar, C-pillar, roof rail, rocker, front header, and roof bow components) have the greatest influence on the roof crush performance, the boundary cuts are made such that the important parts of these components are included in the sub-model.

In order for the boundary constraints to be extracted from the global model and imposed in the sub-model, node sets need to be created that contain the boundary cut edges (interface boundaries) in both the global and local models. The displacements and rotations of the nodes in these sets then need to be extracted from the global model. The sub-model can then have these displacements and rotations applied to the nodes located in its boundary cut node sets. Note that COMPOSE automates this boundary constraint mapping from the global to the sub-model with the process discussed in the next section. Figure 6 shows the sub-model with the boundary constraints imposed for the roof crush study.

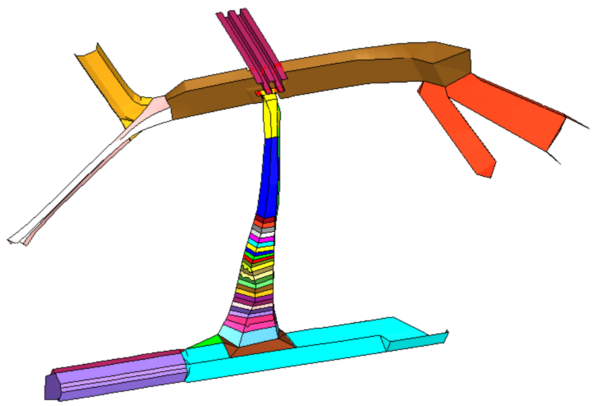

Fig.5. *Roof crush sub-model.*

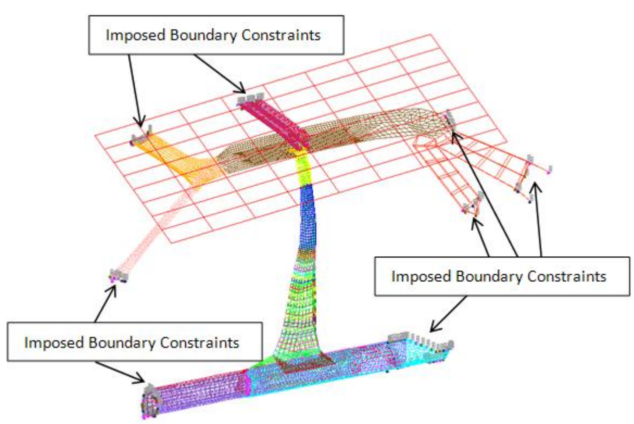

Fig.6. *Roof crush sub-model with boundary constraints highlighted. Cuts were made along the rocker, a-pillar, front header, c-pillar, roof rail, and roof bow components, as shown.*

The COMPOSE Module

The optimization process with COMPOSE is broken down into four basic steps. First, the global system is evaluated using initial values of design variables to determine the boundary conditions at the boundary cut edges. Second, the boundary conditions found in the first step are applied to the sub-system model. Third, the sub-system optimization uses the updated boundary conditions. The optimization contains constraints specific only to the decomposed sub-system. The values of the subsystem design variables will ultimately change, which will strongly affect the overall system if large coupling exists. Finally, the global system is evaluated and a new set of boundary conditions is extracted.

This process is repeated until convergence between the sub-system and global system results is obtained and an optimized global design is found. Figure 7 shows the process COMPOSE uses in the roof crush optimization.

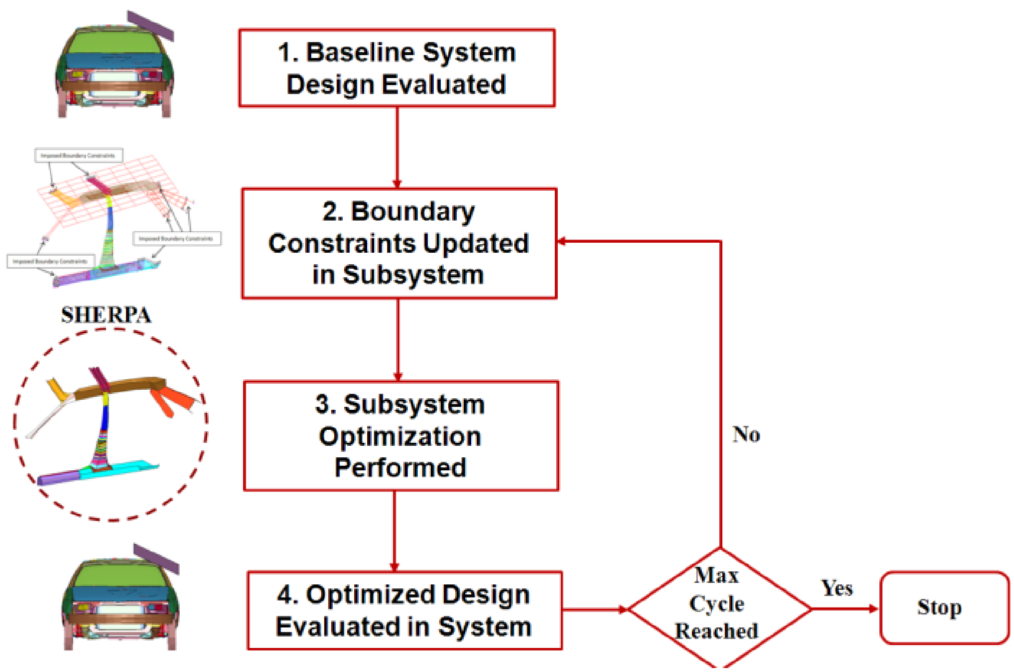

Fig.7. *COMPOSE flowchart for the roof crush optimization*

Roof Crush Optimization Problem Description

The goal of the roof crush optimization was to minimize the mass of the vehicle while satisfying a constraint such that the reaction force was greater than 3.5 times the gross-vehicle weight of the vehicle. This was to be achieved by varying the thicknesses of the critical boron-alloyed steel structural components (A-pillar, B-pillar, roof rail, rocker, front header, and roof bow as shown in Figure 3), as well as the length and location of the non-geometric trigger in the B-pillar.

The optimization problem statement for the roof crush optimization performed in this study can be written as follows:

Objective: Minimize *Mass*

Such That: *Reaction Force* ≥ 68.98 kN

By Varying: 50 mm ≤ *Soft Zone Length* ≤ 200 mm
100 mm ≤ *Soft Zone Max. Ht.* ≤ 575 mm
0.6 mm ≤ *A-pillar Thickness* ≤ 3.0 mm
0.6 mm ≤ *B-pillar Top Thick.* ≤ 3.0 mm
0.6 mm ≤ *B-pillar Thickness* ≤ 3.0 mm
0.6 mm ≤ *Roof Rail Thickness* ≤ 3.0 mm
0.6 mm ≤ *Front Header Thick.* ≤ 3.0 mm
0.6 mm ≤ *Roof Bow Thickness* ≤ 3.0 mm
0.6 mm ≤ *Rocker Thickness* ≤ 3.0 mm

With hot-stamped boron-alloyed steel parts, a soft region can be strategically placed in the part, where the material properties of that region are significantly degraded (or softened). By designing the location and length of this soft region in a B-pillar, a non-geometric trigger can be created to increase performance in the vehicle by forcing desired deformations in the B-pillar. Along with the soft zone, a transition zone exists where the material properties are between the base material and the soft zone in the part. The transition zone in this study was assumed to be a constant 25 mm, and the material properties of this zone were set to the average of the soft zone and the ultra-high-strength zone (see Figure 9).

Figure 8 shows the B-pillar utilized in this study and how the soft zone was designed. Along the length of the B-pillar, multiple parts (components) were created, each with a length of roughly 20 mm. Based upon the location and length of the soft zone, the appropriate material property was assigned to the given B-pillar part.

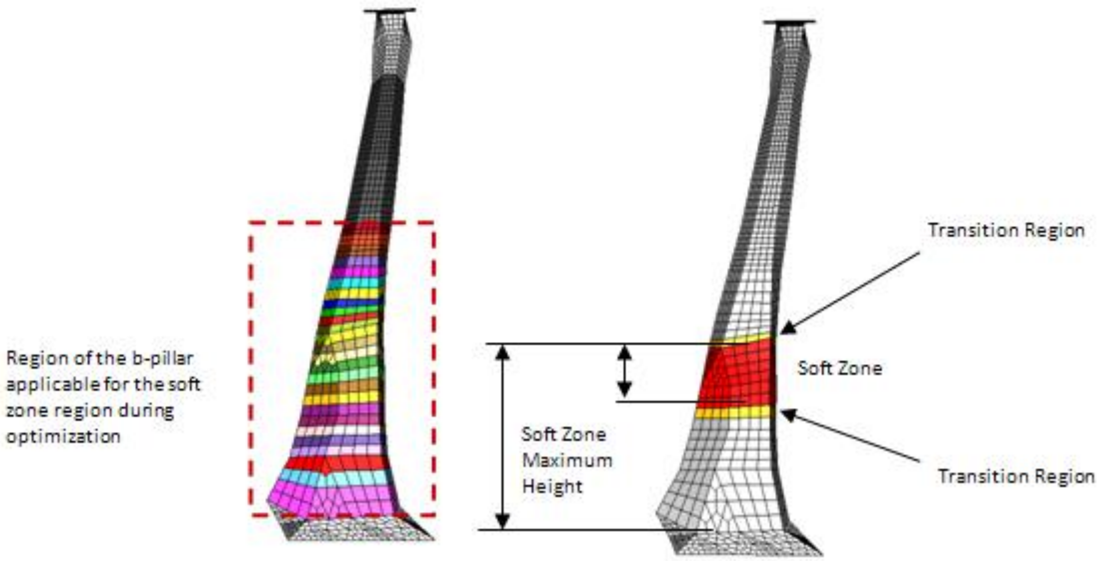

a. B-pillar model used for the roof crush optimization.

b. Example of the soft zone and transition zones that were designed during optimization.

Fig.8. *B-pillar soft zone design technique to introduce a non-geometric trigger.*

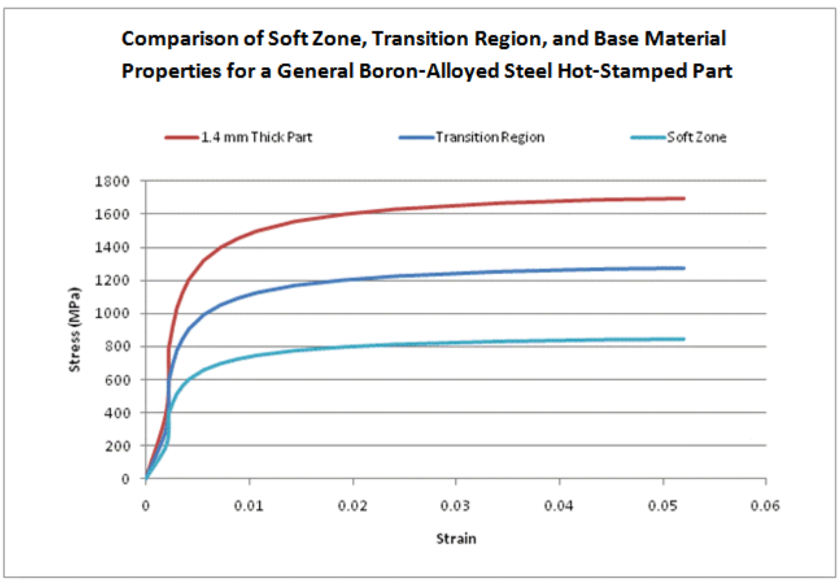

Fig. 9. *Impact of the soft zone region for hot-stamped boron-alloyed steel parts. The difference in material properties can cause a non-geometric trigger in a b-pillar automotive part undergoing impact.*

Optimization Results using COMPOSE

COMPOSE was utilized to optimize the system. The HEEDS MDO run was setup such that 120 sub-system evaluations were performed for every 1 system level evaluation, utilizing the COMPOSE feature and SHERPA as the search method. Eleven such cycles were performed during the optimization, for a total of 12 global system level evaluations and 1,320 sub-system evaluations.

Three such optimizations were performed using COMPOSE; each with a different baseline (starting) design. The goal of performing multiple COMPOSE studies, each with a different starting design, was to show the robustness of this approach. Table 1 shows the starting designs for the three separate COMPOSE optimizations. A description of the designs selected is provided below:

Baseline design 1 – This is a very high mass design and was selected to simulate the scenario where no engineering effort has been spent up front to try to find a reasonable design. All the thickness variables were set to their maximum values for this design.
Baseline design 2 – This is a medium mass design and was selected to simulate the scenario where some engineering judgment has been used to try to reduce the mass for the starting design.
Baseline design 3 – This is a very good starting design with low mass and was selected to simulate the situation where a decent amount of engineering effort has been spent to try to find a good design solution. The mass is close to the best design mass.

All three optimizations performed utilizing COMPOSE found very good designs. Table 2 provides a comparison between the baseline and optimized designs from the three COMPOSE optimization studies. The first optimization found a 43% reduction in mass over the baseline design, while the second optimization found a 51% reduction in mass, and the third optimization found a 31% reduction in mass. All three optimized designs met the reaction force criteria for the roof crush.

Table 3 and Figures 10-12 compare the baseline and optimized design features from the three optimizations. For all three optimizations not only were the gauges of the designable components modified, but the non-geometric trigger location was modified as well. The optimized designs from the second and third optimizations were very similar in performance and design characteristics, while the optimized design from the first optimization was quite different in performance and its design. Figure 13 compares the reaction force profiles for the baseline and optimized designs from all three optimizations.

COMPOSE is an iterative optimization process. Since the boundary conditions of the baseline design drive the optimization process in the first iteration of the optimization, this design has some impact of the search progress. When the starting design is grossly overdesigned, it can take COMPOSE a few more cycles to find a near optimal solution. This is noticed in the first COMPOSE run, where the baseline design is set to the maximum thickness for all the parts and as a result has a very high mass value. COMPOSE is able to do a fairly good job in getting the solution mass down by 43% compared to the baseline, but still heavier when compared with the solutions for the other two runs.

All three runs were setup to perform 11 cycles of search. The third optimization was stopped prematurely after five cycles since the best design found by the run up to that point had a similar performance as that of the best design from the second optimization, and in addition we ran into time and resource constraints. Figure 14 shows plots of the mass of the global system at the end of each COMPOSE cycle for the three different runs. You can see that the starting mass is very different for the three runs, as mentioned earlier in the paper. The plot shows that COMPOSE is able to quickly start reducing the mass of the system in all three cases. The plot also shows that even when a design from the sub-model optimization is evaluated as infeasible in the system model, COMPOSE continues to make progress in the search. Also notice that the closer the solution is in mass to the best solution, the faster COMPOSE is able to find the optimized design. In the first optimization study, since the mass of the system is very high, it would take COMPOSE a few more iterations to find the optimized design.

Table 1. *Baseline designs utilized for 3 separate COMPOSE optimization runs.*

Baseline Design Parameters	**Optimization 1**	**Optimization 2**	**Optimization 3**
Soft Zone Length (mm)	125	175	61
Soft Zone Max. Ht.	300	200	486
A-pillar Thickness	2.5	2.0	1.3
B-pillar Top Thick.	2.5	2.2	1.9
B-pillar Thickness	3.0	2.9	2.8
Roof Rail Thickness	2.5	1.5	1.0
Front Header Thick.	3.0	2.5	2.0
Roof Bow Thickness	3.0	2.5	1.9
Rocker Thickness	2.5	2.0	1.0

Table 2. *Comparison between the performance of the baseline starting designs and the COMPOSE optimized sub-system designs; when put back into the global system level analysis model.*

Optimization	Design	Designable Mass (kg)	Reaction Force (kN)	Mass Reduction
1	Baseline	38.50	105.30	-
	Optimized with COMPOSE	21.84	82.02	43.27 %
2	Baseline	30.63	86.44	-
	Optimized with COMPOSE	14.94	72.26	51.22 %
3	Baseline	22.61	76.05	-
	Optimized with COMPOSE	15.58	70.75	31.09 %

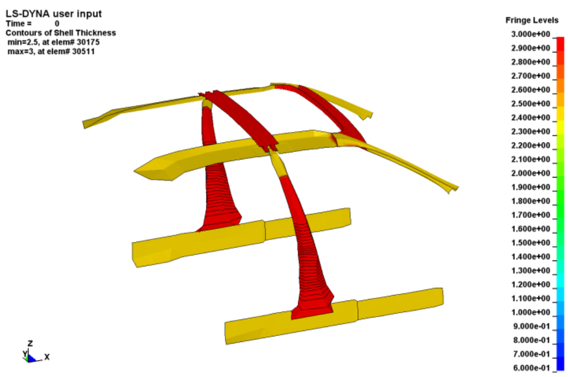

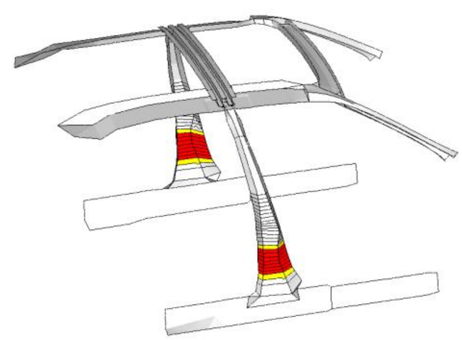

a. *Baseline thickness of designable components (mm).* ***b.*** *Baseline non-geometric trigger location.*

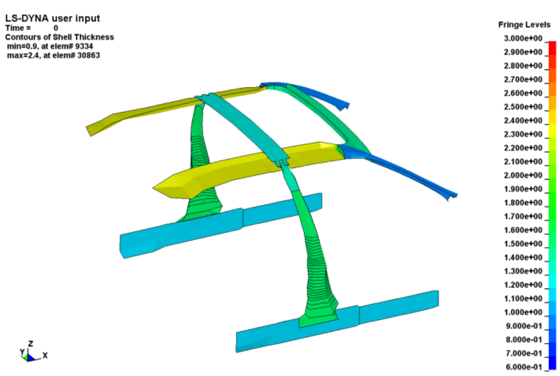

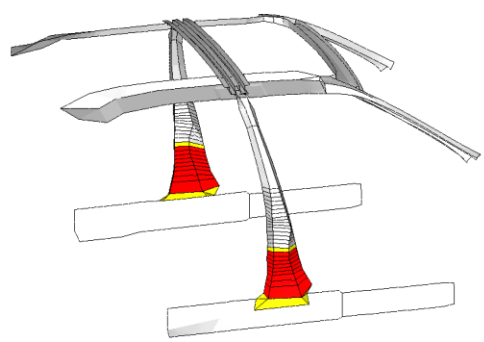

c. *Optimized thickness of designable components (mm).* ***d.*** *Optimized non-geometric trigger location.*

Fig.10. *Comparison between the baseline and optimized design features for optimization 1 using COMPOSE (43% mass reduction).*

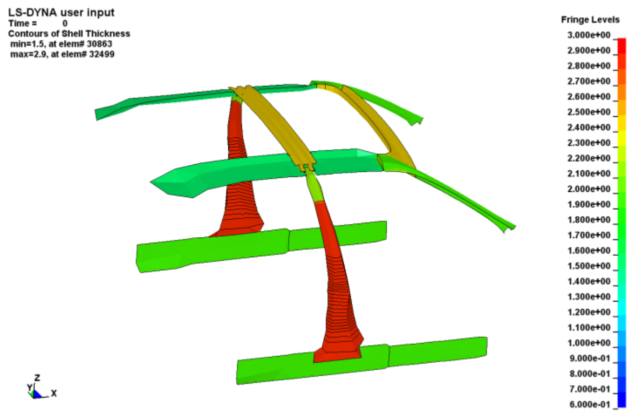

a. *Baseline thickness of designable components (mm).*

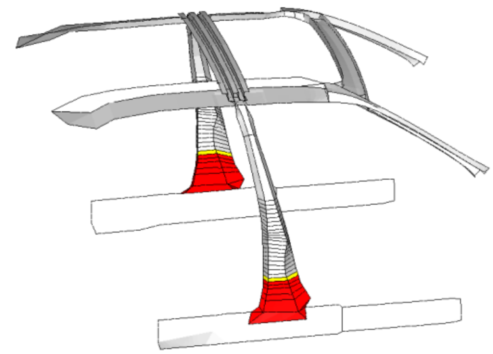

b. *Baseline non-geometric trigger location.*

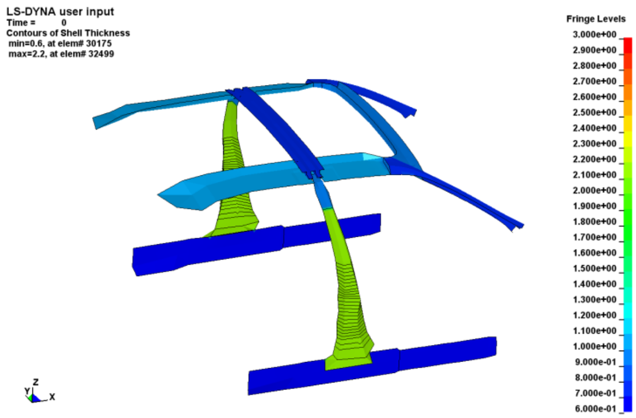

c. *Optimized thickness of designable components (mm).*

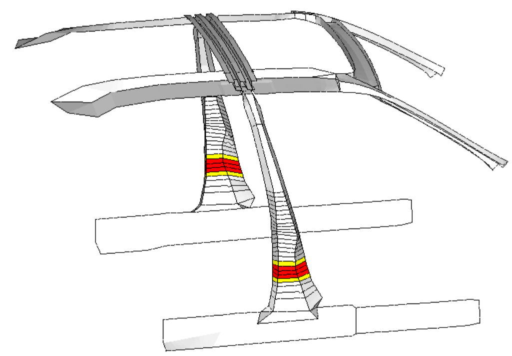

d. *Optimized non-geometric trigger location.*

Fig.11. *Comparison between the baseline and optimized design features for optimization 2 using COMPOSE (51% mass reduction).*

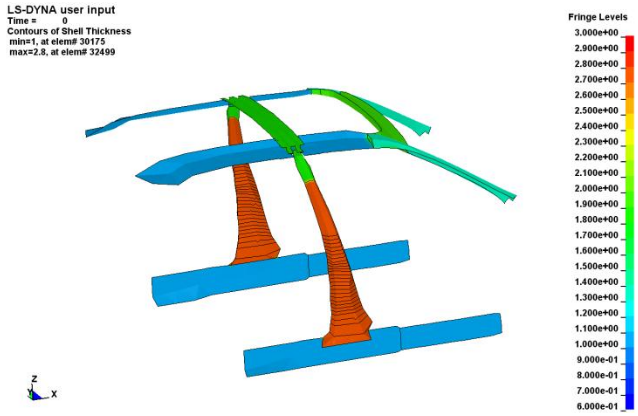

a. *Baseline thickness of designable components (mm).*

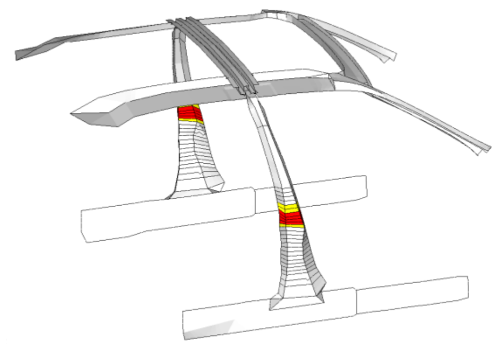

b. *Baseline non-geometric trigger location.*

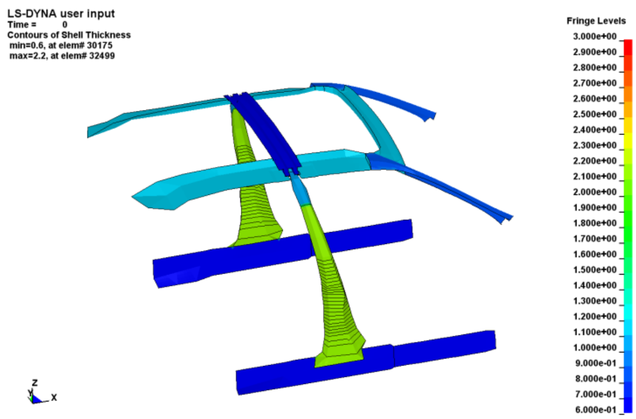

c. *Optimized thickness of designable components (mm).*

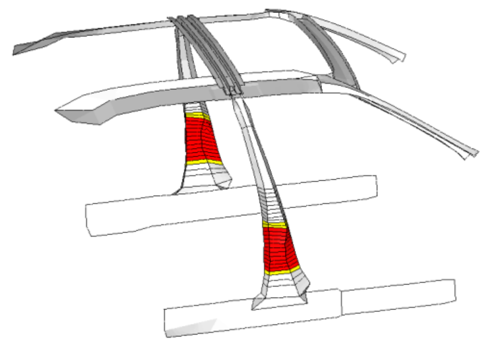

d. *Optimized non-geometric trigger location.*

Fig.12. *Comparison between the baseline and optimized design features for optimization 2 using COMPOSE (31% mass reduction).*

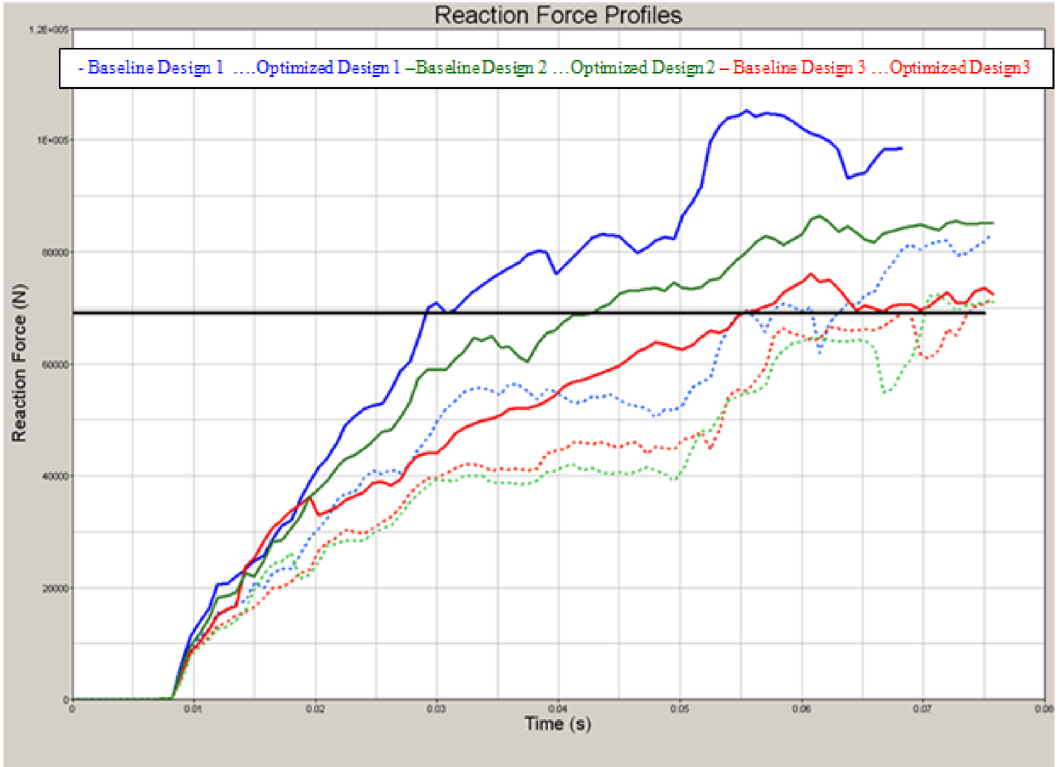

Fig.13. *Comparison of reaction force profiles between the baseline and optimized designs for all three COMPOSE optimizations.*

Table 3. *Optimized design variable values for the optimized designs, compared to the baseline designs.*

Optimization	**1**		**2**		**3**	
Design Variable	**Baseline (mm)**	**COMPOSE Optimized (mm)**	**Baseline (mm)**	**COMPOSE Optimized (mm)**	**Baseline (mm)**	**COMPOSE Optimized (mm)**
Soft Zone Length	125	199.7	175	54.4	61	198.4
Soft Zone Max Height	300	280.5	200	258.3	486	397.7
A-pillar Thickness	2.5	0.9	2.0	0.7	1.3	0.8
B-pillar Top Thickness	2.5	1.3	2.2	0.9	1.9	1.0
B-pillar Thickness	3.0	1.5	2.9	2.2	2.8	2.2
Roof Rail Thickness	2.5	2.4	1.5	1.0	1.0	1.1
Front Header Thickness	3.0	1.4	2.5	0.9	2.0	1.1
Roof Bow Thickness	3.0	1.2	2.5	0.7	1.9	0.6
Rocker Thickness	2.5	1.1	2.0	0.6	1.0	0.6

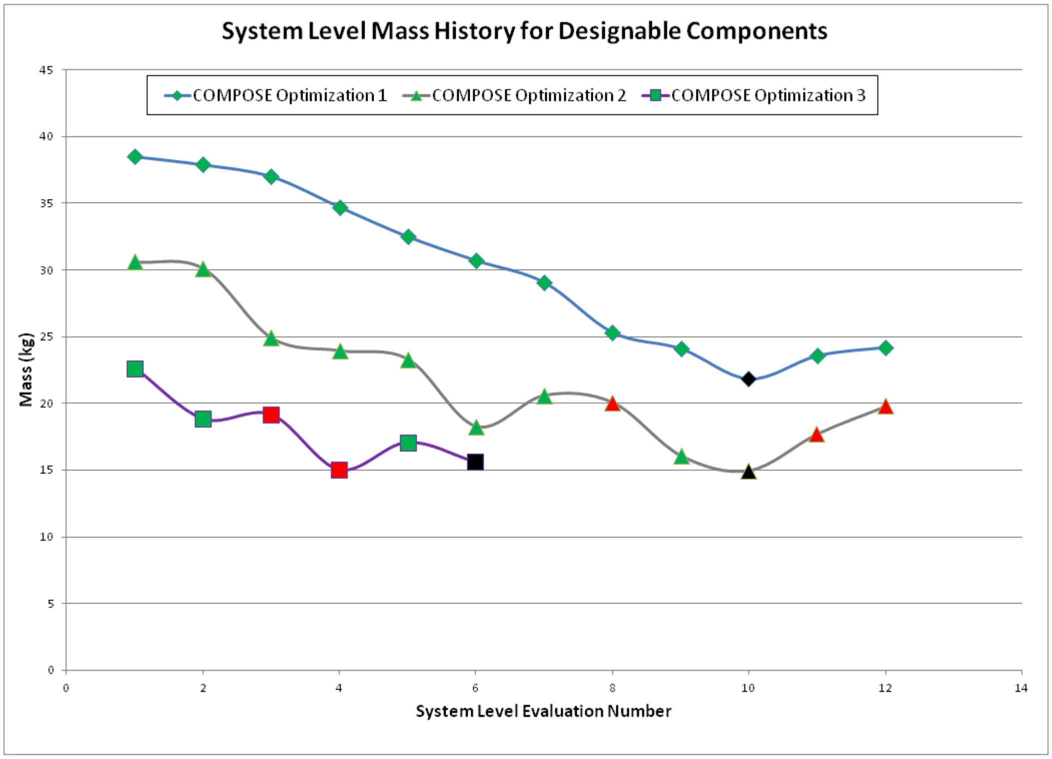

Fig.14. *Mass history plot for the three COMPOSE optimizations showing the mass of the system level designs for each COMPOSE cycle. The green data points represent feasible designs, the red data points infeasible designs (reaction force below specified target), and the black data point marks the best design for each run. Note that the third optimization was stopped after five local optimization cycles since the best design from this run was very close to the optimal solution and we ran into time and resource constraints.*

Optimization Results Using Only a Sub-modeling Optimization Approach

The final part of the study analyzes the level of coupling between the global and the sub-system model. If there is no coupling or a very small amount of coupling between the two models, then the optimization could be performed at the sub-system level without needing to perform any iterations at the global model. This information cannot be calculated a priori without performing some additional sub-system and system evaluations. Even in this case, the actual test is only meaningful at the final optimized design. Typically for a complex global model, the choice of the sub-model that will provide a computational advantage will create significant coupling between the system and the sub-system.

To test whether a simple sub-system level optimization would yield similar results in this problem, we performed optimization studies using the three baseline models in the COMPOSE runs. The details of the three designs used have been provided in Table 1 earlier. The system level boundary constraints for the given baseline design were utilized for all designs evaluated within the given optimization as would be done with a classical sub-system optimization.

The sub-system optimizations were each allowed to perform 250 evaluations using HEEDS MDO as the optimization tool and SHERPA as the search method. The optimized designs at the subsystem level met the reaction force constraint, while reducing the mass of the designable components significantly. However, when these optimized designs were then evaluated at the system level, the performance decreased significantly. The optimal designs in two out of the three studies did not meet the force constraint. As a result, these designs are not acceptable. The constraint was violated by a large amount. Figure 15 compares the reaction forces of the baseline designs with the optimized designs from the subsystem only optimization.

Table 4 compares the system level performance of the baseline designs from the three optimizations with the optimized designs when utilizing COMPOSE vs. utilizing a classical sub-system optimization approach, while Table 5 compares the design characteristics. The fact that the optimized designs from the classical sub-system optimizations did not perform as intended for two of the three optimizations when re-evaluated in the system level analysis model, is an indication that there is significant boundary constraint coupling for this roof crush problem. The fact that all of the optimized designs found by COMPOSE do perform as intended in the system level analysis model, is an indication that COMPOSE is able to maintain the coupling between the system and the sub-system, which increases the robustness of this technique. COMPOSE can be used to solve problems that historically have been unsolvable due to time constraints (large system level optimizations) and coupling limitations (subsystem optimizations).

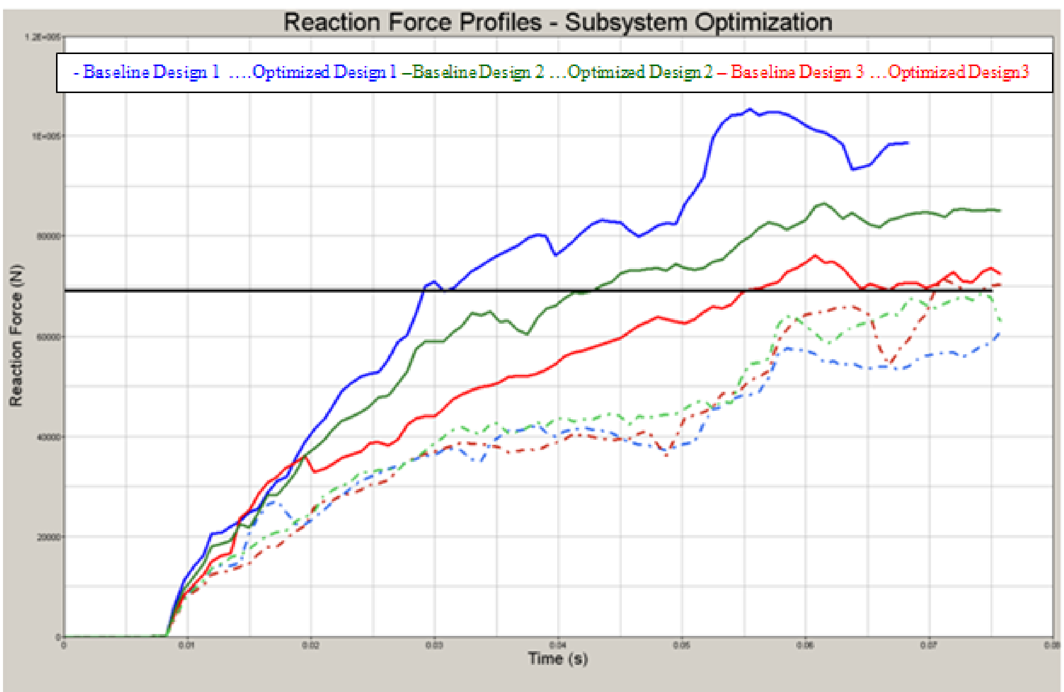

Fig.15. *Comparison of reaction force profiles between the baseline and optimized designs for all three optimizations performed using a subsystem only optimization approach. The optimized design from the second optimization met the reaction force constraint when put back in the system model, while the other two optimized designs did not meet the performance constraint.*

Table 4. *Comparison between the performance of the baseline starting designs, the COMPOSE optimized sub-system designs, and the subsystem only optimized sub-system designs; when put back into the global system level analysis model.*

Optimization	Design	Designable Mass (kg)	Reaction Force (kN)	Mass Reduction
1	Baseline	38.50	105.30	-
	Optimized with COMPOSE	21.84	82.02	43.27 %
	Optimized with Sub-system Only	13.23	60.79	-NA-
2	Baseline	30.63	86.44	-
	Optimized with COMPOSE	14.94	72.26	51.22 %
	Optimized with Sub-system Only	14.15	68.5	-NA-
3	Baseline	22.61	76.05	-
	Optimized with COMPOSE	15.58	70.75	31.09 %
	Optimized with Sub-system Only	16.06	71.29	28.97 %

Table 5. *Optimized design variable values for the optimized designs from COMPOSE and a classical sub-system optimization, compared to the baseline designs.*

Optimization	1			2			3		
Design Variable	Baseline (mm)	COMPOSE Optimized (mm)	Subsystem Only Optimized (mm)	Baseline (mm)	COMPOSE Optimized (mm)	Subsystem Only Optimized (mm)	Baseline (mm)	COMPOSE Optimized (mm)	Subsystem Only Optimized (mm)
Soft Zone Length	125	199.7	61.7	175	54.4	94.5	61	198.4	174.4
Soft Zone Max Height	300	280.5	521.2	200	258.3	571.8	486	397.7	464.2
A-pillar Thickness	2.5	0.9	0.8	2.0	0.7	0.7	1.3	0.8	0.7
B-pillar Top Thickness	2.5	1.3	2.5	2.2	0.9	0.6	1.9	1.0	1.0
B-pillar Thickness	3.0	1.5	0.6	2.9	2.2	1.0	2.8	2.2	2.6
Roof Rail Thickness	2.5	2.4	1.6	1.5	1.0	1.4	1.0	1.1	1.0
Front Header Thickness	3.0	1.4	0.6	2.5	0.9	1.4	2.0	1.1	0.6
Roof Bow Thickness	3.0	1.2	0.7	2.5	0.7	0.8	1.9	0.6	0.8
Rocker Thickness	2.5	1.1	0.6	2.0	0.6	0.6	1.0	0.6	0.7

Conclusions

It was shown here that the use of COMPOSE can yield high-performing designs for roof crush optimization in a way that can significantly reduce the overall optimization time by maintaining the coupling between the subsystem and the global system. COMPOSE makes it possible to optimize large system models efficiently. In the past, these models would have required an impractical amount of compute resources and time for system model optimizations. COMPOSE provides a very efficient and robust technique for optimizing large system models.

References

[1] LS-DYNA (Version 971) [Computer software]. Livermore, CA: Livermore Software Technology Corporation.

[2] HEEDS MDO (Version 6.0) [Computer software]. East Lansing, MI: Red Cedar Technology.

[3] National Crash Analysis Center. Ford Taurus, Modified Model (28,400 elements). http://www.ncac.gwu.edu/
vml/models (accessed January 23, 2012).

[4] Center for Precision Forming, The Ohio State University. 2007. Hot-stamping boron-alloyed steels for automotive parts. *Stamping Journal* January 2007: 14-15. Available online: http://nsmwww.eng.ohio-state.edu/Jan07RDUpdate.pdf (accessed January 23, 2012).

[5] Merklein, M., Lechler, J, and Geiger, M., Characterisation of the Flow Properties of the Quenchenable Ultra High Strength Steel 22MnB5, Annals of the CIRP, Vol. 55, 2006, Kobe, Japan